How Different are UWB Channels From Conventional Wideband Channels?

Ulrich Schuster and Helmut Bölcskei
Communication Technology Laboratory
Swiss Federal Institute of Technology (ETH), CH-8092 Zurich
email: {schuster, boelcskei}@nari.ee.ethz.ch

***Abstract*—We present results of two indoor ultra-wideband (UWB) channel measurement campaigns in the 2 GHz–5 GHz frequency band, and use these results to assess the differences and commonalities between UWB channel models and commonly used indoor wideband channel models. We find that the small-scale fading distributions of the UWB channel impulse response taps can still be adequately modeled as complex Gaussian, with a mean component that depends on the measurement setting. The taps are correlated, although the (frequency) diversity order scales linearly with bandwidth. The power-delay profile typically contains several clusters.**

I. Introduction

Ultra-wideband (UWB) communications is a promising technology to complement wireless local area networks (WLANs) and 3G cellular systems. The bandwidth of UWB systems is two orders of magnitude larger than the bandwidth used in existing wideband systems like WLANs. It is therefore not clear if conventional wideband channel models are suitable to characterize UWB channels. We address this question on the basis of two UWB indoor channel measurement campaigns in the frequency band from 2 GHz to 5 GHz. Our main results can be summarized as follows:

- We find that the Rayleigh distribution is still adequate to model UWB channels whose variations result from motion of the antennas. The Ricean distribution provides the best fit for UWB channels between static terminals, where variations of the channel are caused by movements of objects in the environment.
- The channel taps are weakly correlated, although we find the number of *stochastic degrees of freedom*, i.e., the number of independent (frequency) diversity branches, to scale approximately linearly with bandwidth.

Notation: $\mathbb{E}_X$ stands for the expectation with respect to the random variable X. A probability density function (PDF) that depends on a parameter vector $\boldsymbol{\Theta}$ is denoted as $g_{\boldsymbol{\Theta}}$. Estimated quantities are indicated by a hat $\widehat{\ }$. The superscript ^{T} stands for transposition, and ^{H} for conjugate transposition. All logarithms are to the base e.

This work was supported in part by the Swiss *Kommission für Technologie und Innovation (KTI)* under grant 6715.2 ENS-ES, and by the Swiss *Staatssekretariat für Bildung und Forschung* as part of the Integrated Project PULSERS under contract FP6-506897.

II. Channel Model

Throughout this paper, we restrict our attention to small-scale fading only, and assume that the channel is linear block-wise time-invariant, thereby ignoring Doppler dispersion. As the effective channel, i.e., the physical channel in conjunction with transmit and receive filters, is always band limited, it can be described in terms of samples $h[l]$, called *channel taps*, of the effective continuous-time impulse response $h(\tau)$. Therefore, we consider the discrete-time complex baseband-equivalent channel with input-output relation

$$y[n] = \sum_{l=0}^{L-1} h[l]s[n-l] \tag{1}$$

where $s[n]$ denotes the transmitted signal, and $y[n]$ is the resulting output signal. The input-output relation for indoor wideband communication channels is typically described by (1), where the channel vector $\mathbf{h} = [h[0]\, h[1] \cdots h[L-1]]^T$ is modeled as a random vector with the following properties: (i) $\mathbf{h}$ has $L \lesssim 20$ taps; (ii) each tap $h[l]$ is circularly symmetric complex Gaussian distributed, so that $|h[l]|$ is *Rayleigh* distributed; (iii) if a strong direct path between transmitter and receiver exists, $h[0]$ is typically modeled to have nonzero mean, so that $|h[0]|$ is *Ricean* distributed; (iv) the power-delay profile (PDP) $\mathbb{E}[|h[l]|^2]$ decays exponentially; (v) the taps are statistically independent; (vi) the number of independent taps, and hence the diversity order of the channel, increases linearly with bandwidth W.

UWB channels can also be modeled using the input-output relation (1), because the channels are linear, and the input signals are band limited. However, modeling assumptions (ii), (v), and (vi) are questionable: The time resolution is high, so that the number of partial waves contributing to each tap $h[l]$ might be so small that the central limit theorem can no longer be invoked to justify the complex Gaussian modeling assumption for the distributions of the individual taps [1], [2]. Nakagami [2], lognormal [3], and Weibull [4] distributions have been proposed as alternatives to the Rayleigh and Rice distributions to model UWB channel tap amplitudes. The modeling assumption (v) requires $h[l]$ to be discrete-time uncorrelated scattering (US), which in turn requires an arbitrarily rich scattering environment for $W \to \infty$. But if the $h[l]$ are statistically dependent, the number of stochastic degrees of freedom, i.e., the diversity order, may scale sublinearly with bandwidth.

III. The Channel Measurement Campaigns

We conducted two different UWB channel measurement campaigns to characterize the small-scale fading behavior of channels for different UWB application scenarios. Both campaigns were carried out in the lobby of the ETZ building at ETH Zurich, a typical public open space environment. The lobby has large windows over the entire length on one side, and concrete walls, covered by metal plates, on the opposite side. A row of concrete columns in parallel to the windows partially obstructs the direct path between transmitter and receiver in some of the measurement settings. The measurement campaigns are described in detail in [5].

1) Measurement Campaign I (MC I): In wireless access point scenarios, e.g., for UWB-enhanced 3G terminals or short-range peer-to-peer systems, the terminals move with respect to the environment. To assess the impact of the corresponding spatial variations on the channel, we fixed the position of the receive antenna, moved the transmit antenna on a rectangular 9×5 grid with uniform spacing of 7 cm in both dimensions, displaced the grid by approximately 50 cm, and repeated the procedure. For each of the $N = 90$ antenna locations, we recorded 1601 frequency points in the band from 2 GHz to 5 GHz, using an HP 8722D vector network analyzer. We took measurements with distances d between transmitter and receiver of up to 27.4 m, for line-of-sight (LOS), obstructed LOS (OLOS), and non-LOS (NLOS) settings. Both transmitter and receiver were equipped with a prototype version of the Skycross SMT-3TO10M UWB antenna. We took the measurements at night to ensure a static channel.

The bottom graph in Fig. 1 shows the PDP, obtained by averaging over all 90 recorded impulse responses, for the LOS setting with distance $d = 21.7\,\mathrm{m}$. The PDP and all corresponding impulse responses are "dense", i.e., there are no empty taps as implied by the model in [6]. We can observe several clusters protruding from the otherwise linearly (in dB) decaying PDP. The delay relative to the first arrival, called *excess delay*, of prominent clusters matches the path distance of major reflections, e.g., from the windows, and thus indicates that these clusters presumably result from such reflections.

2) Measurement Campaign II (MC II): In wireless personal area networks and wireless sensor networks, e.g., for building automation or industrial applications, the terminals are typically static, and variations in the channel are mainly caused by moving scatterers, like moving persons. To characterize the corresponding channel statistics, we fixed the position of the transmit and the receive antenna, sounded the channel with a pseudonoise sequence clocked at 10 GHz, and recorded the received signal in real time with the digital sampling oscilloscope Agilent DSO81204A at a sampling rate of 40 GHz and an analog bandwidth of 12 GHz. Through postprocessing as described in [5], we extracted sample impulse responses in the frequency band from 2 GHz to 5 GHz. We acquired $N = 1011$ samples in the LOS setting, with $d = 20\,\mathrm{m}$, $N = 2722$ samples in the OLOS setting, also for $d = 20\,\mathrm{m}$, and $N = 1256$ samples in the NLOS setting, with $d = 13\,\mathrm{m}$. Measurements were taken at daytime, with many people present in the lobby. The PDPs obtained in MC II are less smooth than the PDPs in MC I. This can be seen, e.g., for the OLOS setting, in the bottom graph in Fig. 2. An explanation for this difference is the presence of a strong mean component in the MC II impulse responses.

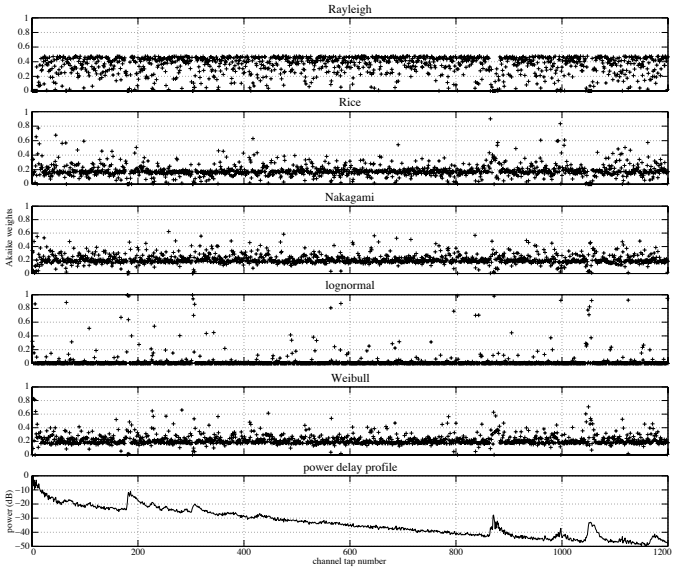

Fig. 1. Akaike weights and PDP for MC I LOS, $d = 21.7\,\mathrm{m}$.

IV. Tap Statistics

1) Model Selection: The main goal in statistical channel modeling is to select, from a set of candidate distributions, a probability model for the channel taps $h[l]$ that approximates as closely as possible the operating model, defined as the nearest representation of the true situation that can be constructed by means of a probability model [7]. A good model should be based on *physical insight*, be *mathematically tractable*, and lead to *consistent predictions*. A measure of approximation quality between a candidate distribution and the distribution of the operating model is called a *discrepancy* [7]. Akaike's Information Criterion (AIC) is an approximately unbiased estimator of the expected Kullback-Leibler discrepancy [8] between a candidate model j ($j = 1, 2, \ldots, J$) with PDF $g^j_{\boldsymbol{\Theta}}$ and the operating model, given as [9]

$$\mathrm{AIC}_j = -2 \sum_{n=1}^{N} \log g^j_{\widehat{\boldsymbol{\Theta}}}(x_n) + 2U \tag{2}$$

where $\widehat{\boldsymbol{\Theta}}$ indicates the maximum-likelihood (ML) estimate of the U-dimensional parameter vector $\boldsymbol{\Theta}$ of the respective PDF, and N stands for the number of samples x_n. AIC provides a relative measure of fit within the candidate set, with the minimum AIC value indicating the best fit. We define the AIC differences $D_j = \mathrm{AIC}_j - \min_i \mathrm{AIC}_i$, where $\min_i \mathrm{AIC}_i$ denotes the minimum AIC value over all J candidate distributions. The *Akaike weights* [10]

$$w_j = \frac{e^{-\frac{1}{2}D_j}}{\sum_{i=1}^{J} e^{-\frac{1}{2}D_i}}, \qquad j = 1, 2, \ldots, J \tag{3}$$

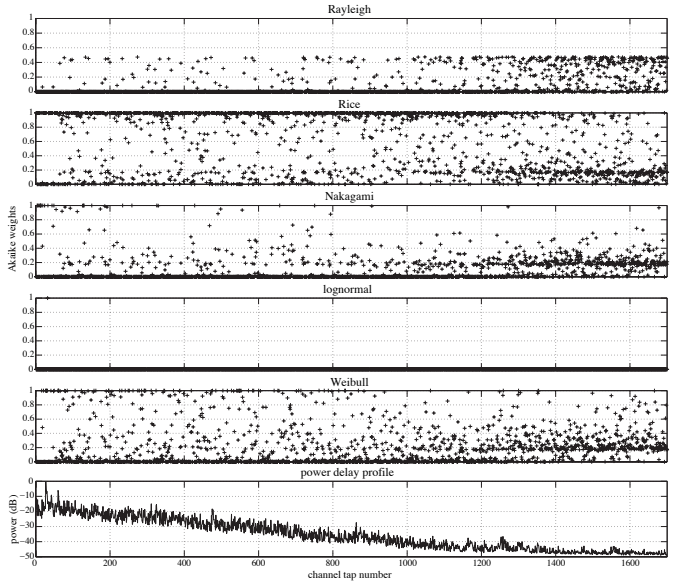

Fig. 2. Akaike weights and PDP for MC II OLOS, $d = 20\,\mathrm{m}$.

which satisfy $\sum_{j=1}^{J} w_j = 1$, can be interpreted as an estimate of the probability that the PDF $g^j_{\widehat{\mathbf{\Theta}}}$ shows the best fit within the candidate set, given the data $\{x_n\}_{n=1}^{N}$. Hence, the weights w_j provide information about the relative approximation quality of each distribution.

2) Amplitude Statistics: We applied AIC to our measurement data to see if the Rayleigh and Rice distributions are appropriate for UWB channels, or if one of the distributions proposed in [2]–[4] provides a better fit. Our candidate set thus consists of the single-parameter ($U=1$) Rayleigh distribution and the two-parameter ($U = 2$) Rice, Nakagami, lognormal, and Weibull distributions. The Rice, Nakagami, and Weibull distributions contain the Rayleigh distribution as a special case. Rayleigh, Rice, and Nakagami amplitude distributions can be justified based on physical principles [11]. The Weibull and lognormal distributions seem to lack physical support for small-scale fading. Akaike weights and corresponding PDPs are shown in Fig. 1 for the MC I LOS setting with $d = 21.7\,\mathrm{m}$, and in Fig. 2 for the MC II OLOS setting. Our main findings are:

1) The Rayleigh distribution shows the best fit for MC I, followed by the Rice, Nakagami, and Weibull distributions in no particular order. The Ricean distribution shows the best fit for the first 1200 taps in MC II.
2) The lognormal distribution shows a consistently bad fit for both MC I and MC II, with the exception of a few isolated taps in MC I.
3) The variability of the Akaike weights is high across taps.

Interpretation of the Results: A closer look at the parameter estimates $\widehat{\mathbf{\Theta}}_j$ in MC I shows that the variability of the Akaike weights across taps is due to the high sensitivity of w_j to $\widehat{\mathbf{\Theta}}_j$. The parameter estimates of the Rice, Nakagami, and Weibull distributions are close to the values that reduce the respective distributions to the Rayleigh distribution. The fit of the Nakagami, Rice, and Weibull distributions in MC I is evidently not good enough to warrant the additional complexity of these distributions, as quantified by the number of free parameters U.

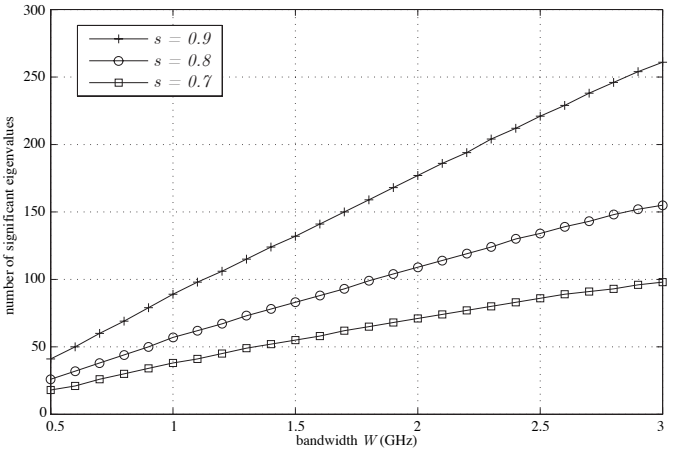

Fig. 3. Number of significant eigenvalues of $\widehat{\mathbf{K}}$ as a function of bandwidth; MC II OLOS setting.

The scattering objects, like windows and walls, that move relative to the position of the antennas in MC I, are quite large, while the moving scatterers in MC II, i.e., people in the lobby, are much smaller. Hence, the major contributions in all taps in MC II are from large static scatterers. Thus, even in an NLOS setting, as long as the antennas are static, fading is best modeled as Ricean, as already observed for narrowband indoor channels [12]. Approximately from tap 1200 on in MC II, the Rayleigh distribution exhibits a better fit than the Ricean distribution. This can be attributed to the low measurement SNR of these taps, so that we are effectively fitting Gaussian distributed noise.

General Comments: Our analysis shows that even for bandwidths of up to 3 GHz Rayleigh and Rice distributions provide a good fit, although the differences of the Akaike weights to the Nakagami and Weibull distributions are often small, especially in MC I. Hence, there seems to be no compelling reason to abandon the simple and analytically tractable Rayleigh and Rice distributions used in typical indoor wideband channel models.

We did not apply model selection tools to determine the distributions of the phases of the complex-valued channel taps, as there does not seem to be a physically motivated alternative to the almost exclusively used uniform phase assumption. The combination of the Rayleigh, respectively Ricean, amplitude distribution with the assumption of a uniformly distributed phase of the zero-mean component results in the complex Gaussian distribution for each individual tap. Marginal Gaussian distributions do not imply joint Gaussianity of the channel vector $\mathbf{h}$. However, selection of the joint PDF of $\mathbf{h}$ using AIC is a hopeless endeavor because of the large number of parameters involved. As we did not find evidence against the joint Gaussianity assumption [5], [13], and again referring to analytical tractability of the model, we advocate the use of the jointly complex Gaussian distribution for $\mathbf{h}$.

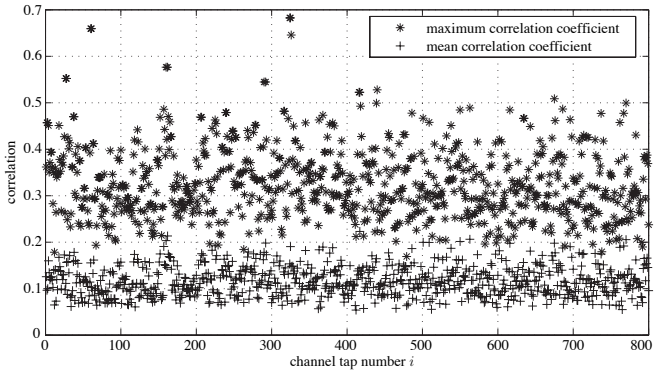

Fig. 4. Maximum and mean channel tap correlation coefficient magnitudes; MC II OLOS setting.

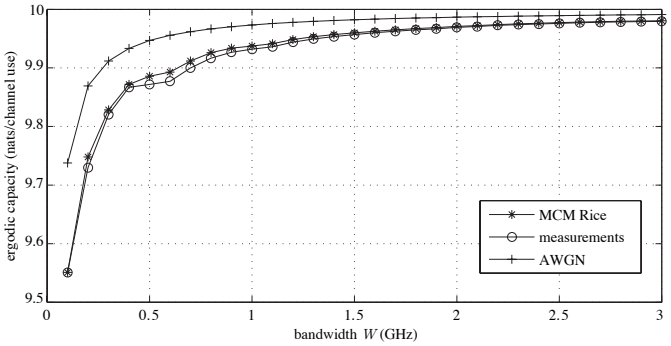

Fig. 5. Estimated ergodic capacity $\widehat{C}$ according to (4) for MC II OLOS data, Monte Carlo estimate of the capacity of the corresponding synthetic channel, and AWGN capacity for comparison, $P/N_0 = 10\,\mathrm{dB}$.

V. The Uncorrelated Scattering Assumption

The correlation between channel taps in the discrete-time model (1) can result from correlated scattering in the underlying continuous-time propagation channel [11], or from the effect of the antennas and the transmit and receive filters. Separating these two sources of correlation on the basis of measurements is difficult. Therefore, we do not attempt to assess the continuous-time US assumption, but consider the discrete-time effective channel only and analyze its intertap correlation.

We decompose the random channel vector $\mathbf{h}$ according to $\mathbf{h} = \mathbf{m} + \tilde{\mathbf{h}}$, with $\mathbf{m} = \mathbb{E}[\mathbf{h}]$. Under the assumption that $\mathbf{h}$ is jointly complex Gaussian distributed with circularly symmetric $\tilde{\mathbf{h}}$, the joint distribution of $\mathbf{h}$ is specified through $\mathbf{m}$ and the covariance matrix $\mathbf{K} = \mathbb{E}\big[\tilde{\mathbf{h}}\tilde{\mathbf{h}}^H\big]$. We truncate all measured impulse responses $\mathbf{h}_n$, $n = 1, 2, \ldots, N$ after $L = 701$ taps (above the noise floor), and compute the empirical $L \times L$ covariance matrix $\widehat{\mathbf{K}} = \frac{1}{N}\sum_{n=1}^{N}(\mathbf{h}_n - \widehat{\mathbf{m}})(\mathbf{h}_n - \widehat{\mathbf{m}})^H$, were $\widehat{\mathbf{m}} = \frac{1}{N}\sum_{n=1}^{N}\mathbf{h}_n$. Accurate estimation of $\mathbf{K}$ requires a large number of samples; hence, we use data from MC II in the following.

The diversity order of a frequency-selective Ricean channel is well-defined, and given by the rank of $\mathbf{K}$ [14]. We denote the kth eigenvalue of $\widehat{\mathbf{K}}$ as $\widehat{\lambda}_k$, use the normalization $\sum_{k=1}^{L}\widehat{\lambda}_k = 1$, and arrange the eigenvalues in decreasing order, i.e., $\widehat{\lambda}_1 \geq \widehat{\lambda}_2 \geq \cdots \geq \widehat{\lambda}_L$. We declare all eigenvalues $\widehat{\lambda}_k$ with index $k \leq L_s$ to be significant, where L_s is the largest integer satisfying $\sum_{k=1}^{L_s}\widehat{\lambda}_k \leq s$, with $0 \leq s \leq 1$. For the OLOS setting Fig. 3 depicts the scaling behavior of the significant eigenvalues as a function of bandwidth W for different s. We observe that the scaling is approximately linear. The corresponding observations for the LOS and NLOS settings are similar.

Linear scaling of the number of significant eigenvalues with bandwidth is not sufficient to conclude that the discrete-time US assumption is satisfied. To refine our analysis, we estimate the correlation coefficients $\widehat{\rho}_{ij} = [\widehat{\mathbf{K}}]_{ij}/\big([\widehat{\mathbf{K}}]_{ii}[\widehat{\mathbf{K}}]_{jj}\big)^{1/2}$, with $i, j = 1, 2, \ldots, L$. Fig. 4 shows the mean correlation coefficient magnitude $\frac{1}{L}\sum_{j=1}^{L}|\widehat{\rho}_{ij}|$, and the maximum correlation coefficient magnitude $\max_j |\widehat{\rho}_{ij}|$ for each $i = 1, 2, \ldots, L$, computed from the first $L = 800$ taps of the $N = 2722$ MC II OLOS impulse responses. We find that the taps are indeed correlated; hence, the discrete-time US assumption is not satisfied for the bandwidth considered.

Finally, we note that sublinear scaling of the number of stochastic degrees of freedom was observed in [15], where a measurement setup similar to MC I was used. This indicates that there might be a fundamental difference between the spatially varying channel measured in [15] and the channel with static terminals in MC II.

VI. Capacity Estimates

The goal of this section is to compare the standard wideband model with uncorrelated Ricean taps to the measured UWB channels from MC II. Our figures of merit are ergodic and outage capacities for perfect channel knowledge at the receiver and no channel knowledge at the transmitter [16].

1) Ergodic Capacity: An estimate of the ergodic capacity on the basis of N samples of $\mathbf{h}$ can be obtained as [17]

$$\widehat{C} = \frac{1}{N}\sum_{n=1}^{N}\sum_{k=0}^{K-1}\log\Big(1 + \frac{P}{KN_0}\,|H_n[k]|^2\Big) \quad \text{[nats/ch. use]} \quad (4)$$

where $\mathbf{H}_n = [H_n[0]\, H_n[1]\, \ldots\, H_n[K-1]]^T$ is the length-K discrete Fourier transform of the nth channel vector sample $\mathbf{h}_n$. The transmit power is constrained to P, allocated uniformly over frequency. N_0 is the noise variance, identical for each of the K parallel subchannels.

Using (4), we estimate the ergodic capacity from the measurement data of MC II, with the channel impulse responses truncated after $L = 701$ taps. Note that this estimate does not assume a specific distribution of the taps, nor does it impose any correlation structure between taps. For comparison, we use the Monte Carlo method (MCM) to estimate the capacity of a synthetic uncorrelated Ricean channel, with mean and variance of each tap equal to the ML-estimate obtained from the measured data. Measured and synthesized impulse responses are normalized to unit average power. The result for the OLOS setting is shown in Fig. 5, where we set $P/N_0 = 10\,\mathrm{dB}$, and used $K = 5608$ tones at $W = 3\,\mathrm{GHz}$. The channel synthesized

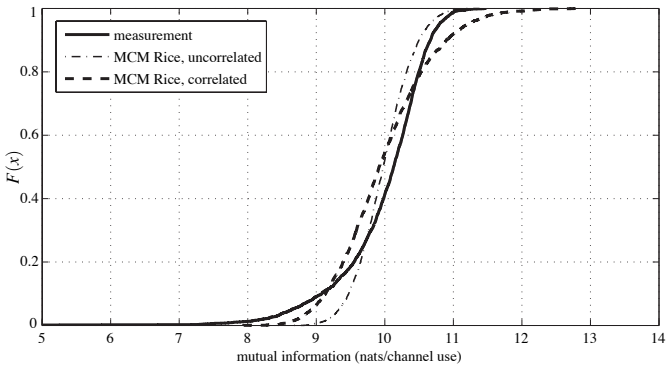

Fig. 6. Empirical CDF of the mutual information for MC II OLOS data, and Monte Carlo estimate of the CDFs for the corresponding synthetic channels; $P/N_0 = 10\,\mathrm{dB}$.

according to the uncorrelated Ricean model accurately predicts the ergodic capacity of the measured channel.

2) Outage Capacity: For slow-fading channels, the mutual information, given as [16]

$$I = \int_{-W/2}^{W/2} \log\Big(1 + \frac{P}{WN_0}\,|H(f)|^2\Big)\,df \quad \text{[nats/ch. use]} \qquad (5)$$

is a random variable, because the channel $H(f)$ is random. In this case, the ϵ-outage capacity C_ϵ, defined as $\mathbb{P}(I < C_\epsilon) \leq \epsilon$, is a more meaningful performance measure than the ergodic capacity [16]. Fig. 6 shows the empirical cumulative distribution function (CDF) of the mutual information $\widehat{I}$, estimated for the measured and two synthesized channels. One of the synthesized channels takes into account intertap correlation according to $\widehat{\mathbf{K}}$. The left tail of the measured CDF is more pronounced compared to the CDFs of the synthetic channels. This might result from people blocking strong reflections, thus shadowing the received signal and degrading the received SNR, which in turn reduces the achievable rate.

VII. Conclusion

We find that the UWB indoor channels we measured are not too different from typical wideband channels. The distribution of the channel taps can still be modeled as complex Gaussian, despite the much larger bandwidth and the corresponding high temporal resolution. The differences in the results between MC I and MC II show that it is important to determine if a UWB communication system will operate with mobile or fixed terminals; this finding, however, is not peculiar to UWB channels [12]. The high temporal resolution reveals clustering effects in the PDP, caused by dominant reflectors. This clustering phenomenon has previously been observed in several other UWB measurement campaigns, e.g., [2], [3].

We find that individual channel taps are correlated, which is different from the standard modeling assumption (v). The correlation is low between most taps, but the maximum correlation coefficient can reach up to 0.7. The impact of intertap correlation on ergodic and outage capacities is difficult to assess, because our measurements do not allow to perfectly separate small-scale fading from shadowing.

Our finding that the number of stochastic degrees of freedom scales approximately linearly with bandwidth in MC II is surprising, as the channel is not strictly US. We note that results from a measurement campaign reported in [15] show sublinear scaling of the number of stochastic degrees of freedom with bandwidth, which indicates that the measurement setting might have a major influence on scaling behavior.

Acknowledgment

The authors would like to thank G. Durisi, who was of great help in MC II, H.-R. Benedickter and C. Schmidt for their support regarding RF measurement and instrumentation issues, and Prof. H.-R. Künsch and his staff for helpful discussions.

References

[1] A. F. Molisch, J. R. Foerster, and M. Pendergrass, "Channel models for ultrawideband personal area networks," *IEEE Wireless Commun. Mag.*, vol. 10, no. 6, pp. 14–21, Dec. 2003.

[2] D. Cassioli, M. Z. Win, and A. F. Molisch, "The ultra-wide bandwidth indoor channel: From statistical models to simulations," *IEEE J. Select. Areas Commun.*, vol. 20, no. 6, pp. 1247–1257, Aug. 2002.

[3] J. Keignart and N. Daniele, "Channel sounding and modelling for indoor UWB communications," in *Proc. Int. Workshop on Ultra Wideband Systems*, Oulu, Finland, June 2003.

[4] P. Pagani and P. Pajusco, "Experimental assessment of the UWB channel variability in a dynamic indoor environment," in *Proc. Int. Symp. Personal, Indoor and Mobile Radio Communications*, vol. 4, Barcelona, Spain, Sept. 2004, pp. 2973–2977.

[5] U. G. Schuster and H. Bölcskei, "Ultra-wideband channel modeling on the basis of information-theoretic criteria," *IEEE J. Select. Areas Commun.*, 2005, submitted.

[6] J. R. Foerster, "Channel modeling sub-committee report final," IEEE 802.15 SG3a, Tech. Rep. P802.15 02/490r1, Feb. 2003.

[7] H. Linhart and W. Zucchini, *Model Selection*. New York, NY, U.S.A.: Wiley, 1986.

[8] K. P. Burnham and D. R. Anderson, *Model Selection and Multimodel Inference—A Practical Information-Theoretic Approach*, 2nd ed. New Nork, NY, U.S.A.: Springer, 2002.

[9] H. Akaike, "Information theory and an extension of the maximum likelihood principle," in *Breakthroughs in Statistics*, S. Kotz and N. L. Johnson, Eds. New York, NY, U.S.A.: Springer, 1992, vol. 1, pp. 610–624, originally published in the *Proceedings of the Second International Symposium on Information Theory*, Budapest, Hungary, 1973.

[10] ——, "On the likelihood of a time series model," *The Statistician*, vol. 27, no. 3/4, pp. 217–235, Dec. 1978.

[11] R. Vaughan and J. B. Andersen, *Channels, Propagation and Antennas for Mobile Communications*. London, UK: The Institution of Electrical Engineers, 2003.

[12] R. J. C. Bultitude, "Measurement, characterization and modeling of indoor 800/900 MHz radio channels for digital communications," *IEEE Commun. Mag.*, vol. 25, no. 6, pp. 5–12, June 1987.

[13] U. G. Schuster, H. Bölcskei, and G. Durisi, "Ultra-wideband channel modeling based on information theoretic criteria," in *Proc. IEEE International Symposium on Information Theory (ISIT)*, Adelaide, Australia, Sept. 2005, submitted.

[14] R. U. Nabar, H. Bölcskei, and A. J. Paulraj, "Diversity and outage performance in Ricean MIMO channels," *IEEE Trans. Wireless Commun.*, 2005, to appear.

[15] R. Saadane, A. Menouni, R. Knopp, and D. Aboutajdine, "Empirical eigenanalysis of indoor UWB propagation channels," in *Proc. IEEE Global Telecommunications Conference (GLOBECOM)*, Dallas, TX, U.S.A., Nov. 2004, pp. 3215–3219.

[16] E. Biglieri, J. Proakis, and S. Shamai (Shitz), "Fading channels: Information-theoretic and communications aspects," *IEEE Trans. Inform. Theory*, vol. 44, no. 6, pp. 2619–2692, Oct. 1998.

[17] H. Bölcskei, D. Gesbert, and A. J. Paulraj, "On the capacity of OFDM-based spatial multiplexing systems," *IEEE Trans. Commun.*, vol. 50, no. 2, pp. 225–234, Feb. 2002.